AIAA Meeting Papers on Disc, July 1996
A9637184, AIAA Paper 96-3036

Deep-cooled turbojet augmented with oxygen (cryojet) for a SSTO launch vehicle

V. V. Balepin
Central Inst. of Aviation Motors, Moscow, Russia

M. Maita
National Aerospace Lab., Tokyo, Japan

N. Tanatsugu
Inst. of Space and Astronautical Sciences, Kanagawa, Japan

S. N. B. Murthy
Purdue Univ., West Lafayette, IN

AIAA, ASME, SAE, and ASEE, Joint Propulsion Conference and Exhibit, 32nd, Lake Buena Vista, FL, July 1-3, 1996

It has been shown in the past that a thermally integrated deep-cooled turbojet and a liquid rocket engine provide an increase in payload fraction up to 2.5 percent compared to a single rocket motor. An issue in deep-cooling is the possibility of ice formation. To overcome that problem and for other reasons, liquid oxygen addition ahead of the precooler seems to offer advantages. A preliminary performance estimate is provided for a combined DCTJ-LRE with modest LOX augmentation. The injected oxygen requirement is small for the problem of icing to be entirely overcome, and a further gain in payload fraction seems possible. (Author)

AIAA-96-3036

DEEP-COOLED TURBOJET AUGMENTED WITH OXYGEN (CRYOJET) FOR A SSTO LAUNCH VEHICLE

V.V. Balepin[1], M. Maita[2], N. Tanatsugu[3],
and
S.N.B. Murthy[4]

Abstract

It has been shown in the past that a thermally integrated deep-cooled turbojet and liquid rocket engine provides an increase in payload fraction up to 2.5% compared to a single rocket motor. An issue in deep-cooling is the possibility of ice formation. To overcome that problem and for other reasons liquid oxygen addition ahead of the precooler seems to offer advantages. A preliminary performance estimate is provided for a combined DCTJ-LRE with modest LOX augmentation. The injected oxygen requirement is small for the problem of icing to be entirely overcome, and a further gain in payload fraction seems possible.

INTRODUCTION

A number of studies have shown the possible benefits of combined ABE-LRE systems for SSTO propulsion[1-4]. Air precooling before compression in a turbofan utilized in high speed flight propulsion systems is an accepted means of improving compression efficiency[5-9]. Deep cooling (below 120 K at sea level conditions) significantly changes the cycles in terms of configuration, performance, and materials. Reference 8 deals with a deep-cooled air-turborocket, with precooling almost to saturation conditions. In Ref. 9 the concept of SSTO propulsion consisting of thermally integrated deep-cooled turbojet and liquid rocket engine has been presented. Such a combined DCTJ-LRE concept is considered as near-term technology since it does not require the sophisticated technologies of, for example, the LACE cycle.

Icing of the Precooler

One of the issues with precooling of air is the possibility of precooler icing, that may cause blockage and otherwise affect engine performance. It was suggested in Ref. 5 that such icing may be avoided provided at least one of the following conditions is satisfied:

- ambient air temperature < 273°k; and
- partial pressure of water vapor is less than that at the triple point.

Figure 1 illustrates the thermodynamic limits from the phase diagram for water. This is based on experimentally confirmed observations on the physical mechanisms involved in ice formation. Given data on seasonal variations of humidity it is, therefore, possible to establish icing-free operational schedules for launches. References 10 and 11 provide further details along with an example.

The example considered was the ATREX engine, and its proposed launch site at Taiki, Japan, along with the proposed flight trajectory. The reference trajectory and the seasonal limits for icing are shown in Fig. 2. The icing process occurs at a high rate from sea level up to a certain altitude, and then at a decreasing rate. In Fig. 2 the partial pressure of water vapor in air under stagnant conditions is less than the triple point pressure above each of the lines for the month indicated, taking account of the humidity data. It can be observed that no icing is expected during the November-April period as the vapor pressure in that period is always less than the triple point pressure. In the July-August period, icing must be expected, and the limit for icing to occur is about 4 km altitude at a flight Mach number of 0.8 for the given flight trajectory. Predictions of a similar type can be established for other launch sites, flight vehicles, and their flight trajectories.

Use of Oxygen Injection

In the current paper, another possibility for entirely overcoming the problem of icing, namely

[1] Institute of Space and Astronautical Sciences, Kanagawa, Japan; currently at Central Institute of Aviation Motors, Moscow.
[2] Science and Technology Agency, National, Aerospace Laboratory, Tokyo, Japan.
[3] Institute of Space and Astronautical Sciences, Kanagawa, Japan.
[4] Purdue University, West Lafayette, IN, USA.

liquid oxygen addition to incoming air ahead of the precooler, is examined. The temperature of air at the precooler can then be reduced as desired, and this precludes the possibility of icing. It has been clear from the conceptual stage that such LOX addition, while leading to a thrust increase, would decrease the specific impulse (relative to on-board propellant usage) compared to the basic DCTJ. Hence, an underlying consideration in the following analysis is to require that the vehicle performance does not become too much affected with oxygen injection compared to the simple case of no LOX injection.

Referring to the example of the ATREX engine, one can consider LOX injection, during the July-August months, from SLS condition to flight Mach 0.8. Based on meteorological data and Fig. 2, one can establish the length of time over which oxygen injection is required along the flight path in those months. Figure 3 shows that the maximum length of time over which LOX injection is required in those months is about 45 s.

INTEGRATED DCTJ-LRE PROPULSION SYSTEM

Figure 4 illustrates a scheme for thermal integration of DCTJ and LRE with oxygen injection in front of the DCTJ precooler. It may be pointed out that the DCTJ and the LRE are expected to operate simultaneously and together from take-off to the highest Mach number desired; in the current study the combined engine is assumed to operate up to flight Mach number 6.0.

At sea level conditions, hydrogen can be utilized in a precooler to chill to near saturation conditions about half the air needed for stoichiometric combustion of hydrogen (roughly, the fraction, 0.5/0.02916). Any further increase in air-to-hydrogen ratio in the precooler causes a significant increase in the precooler size and mass. A limiting value for the ratio is about 18-22 depending on the initial temperature of hydrogen and various other factors. Thus, deep-cooling may necessitate non-stoichiometric engine operation even at sea level conditions when a separately operating precooler is used. The deep-cooled air-turborocket of Ref. 8 is such an engine with air precooling almost to the saturation limit and an air-equivalence ratio (ε) approximately equal to 2.0; the precooler operates as a separate unit, unintegrated with the engines.

In the case of the DCTJ-LRE system under consideration here, in contrast, the precooler has sufficient capacity for cooling the air since it can use the hydrogen needed for both the DCTJ and the LRE in cooling all of the air needed for stoichiometric combustion of hydrogen in the DCTJ, and this leads to increased propulsion performance and, in turn, to a reduced engine mass. This is the benefit of thermal integration of the precooler, as can be observed in Fig. 2, with the thermally integrated DCTJ-LRE unit. In addition to the usual benefit of precooling ahead of turbo-compression, one can also thereby realize the benefits of near-stoichiometric operation of the DCTJ.

A reduction in engine mass also arises for several reasons: i) The difference in temperature between the air and the coolant I the precooler can be of the order of 60 – 100 C. There is no "pinch point" as in the cooler-condenser of a LACE system. ii) The compressor mass is reduced since there is considerable – nearly 1/2.5 – 1/3.0 – reduction in work required for the same compression pressure ratio. iii) Similarly the turbine and the shaft mass are reduced because of the decrease in work output required, and the reduced loading; and iv) possibility of using light aluminum alloys for the precooler and light weight carbon-reinforced composites for the compressor.

Regarding materials, according to Ref. 11, 3.2 mm diameter tubes with a wall thickness of 0.05–0.23 mm were fabricated with aluminum alloy and subjected to structural tests back in the 60's, the maximum test temperature being 811 K for tubes of 0.1 mm thickness. In the current analysis, it is assumed that aluminum alloys are suitable for the entire precooler, noting that in high temperature regimes it may be possible and, perhaps, unavoidable that excess hydrogen is utilized. The precooler is thus an optimized shell and tube type unit with a tube wall thickness of 0.1 mm. Carbon-reinforced plastics of density equal to about 2,000 kg/m^3 are assumed the compressor material.

Performance Estimation with LOX Injection Equivalence Ratio. Considering the combined cycle engine system of Fig. 4, we consider operation with chosen values of air to hydrogen ratio in the DCTJ, k_A, injected oxygen ratio, ϕ, and the ratio of hydrogen supplied to the TJ in relation to the total amount of hydrogen utilized, ξ. The parameters ϕ and ξ may be expressed by the relations

$$\phi = G_{OX} / (G_A + G_{OX}) \qquad (1)$$

and

$$\xi = G_H^{TJ} / G_H^{\Sigma} \tag{2}$$

Introducing the oxygen-to-hydrogen stoichiometric ratio, $k_O(= 7.937)$, and the average oxygen concentration in standard air, $C_O^A(= 0.2315)$, one can consider two parameters as follows:

(i) L_O, the stoichiometric ratio of oxygen in air-oxygen mixture to hydrogen, given by

$$L_O = \frac{k_O G_A}{C_O^A G_A + G_{ox}} \tag{3}$$

$$= \frac{k_O(1-\phi)}{C_O^A + \phi\left(1 - C_O^A\right)}, \tag{4}$$

(ii) ε, the air-to-total hydrogen equivalence ratio, given by

$$\varepsilon = \frac{\xi L_O(1-\phi)}{k_A} \tag{5}$$

Figure 5 provides the mixture stoichiometric ratio and the air-oxygen mixture temperature as a function of the injected oxygen fraction, assuming that the injected oxygen is at 55 K. It can be observed that 4% oxygen addition is adequate to chill standard air at 288 K to below the water triple point.

Total Specific Impulse. We assume that the exhaust velocity is V_j in the DCTJ and k_X is the oxygen-to-hydrogen mixture ratio in the LRE. If the specific impulse of the LRE is written as I_{LRE}, then the specific impulse of the integrated combined cycle engine becomes

$$I_\Sigma = \Big[(1-\xi)(k_X+1)I_{LRE} + k_A\left(V_j - V_O\right) + \xi(1-\phi)V_j\Big] \Big/ \Big[1 + \phi(k_A - 1) + (1-\xi)(1-\phi)k_X\Big] \tag{6}$$

where the velocity of flight is denoted by V_O. The specific impulse is determined with respect to all of the intrinsic (or on-board) propellants utilized.

Turbojet Thrust. The fraction of total thrust generated by the turbojet can be written as

$$R_{TJ} = 1 \Big/ \left[\frac{(1-\xi)(k_X+1)(1-\phi)\cdot I_{LRE}}{\left\{k_A + \xi(1-\phi)\right\}V_j} + 1\right] \tag{7}$$

Propulsion System Specific Mass. The specific mass of the propulsion system is the propulsion system mass per unit of thrust. Writing the mass of the TJ per unit mass/s of airflow through the TJ, m_{TJ}^*, the specific mass of the LRE as γ_{LRE}, and the throttle ratio or factor as ψ, the specific mass of the combined cycle becomes

$$\gamma_\Sigma = \frac{\gamma_{LRE}}{\psi}(1 - R_{TJ}) + \frac{m_{TJ}^*(1-\phi)}{I_\Sigma\left[1 + \phi(k_A - 1) + (1-\xi)(1-\phi)k_V\right]} \tag{8}$$

The mass m_{TJ}^* can be considered to include the mass of the air intake, precooler, turbomachinery, and nozzle.

The throttle ratio denotes the level of throttling: thus $\psi = 0$ denotes that the LRE is non-operative, and $\psi = 1$, that LRE operates at full power.

SSTO VEHICLE WITH OXYGEN-AUGMENTED PROPULSOR

A SSTO vehicle is considered with the overall propulsion system consisting of the combined DCTJ-LRE unit for acceleration from flight Mach 0 to 6.0, and the LRE to provide acceleration thrust to space. In this case the LRE must provide vehicle thrust-to-weight ratio greater than unity in the post-transition flight regime. This requires that either the DCTJ thrust contribution should be limited in the first part of the flight from SLS condition to flight Mach 6.0, or a separate LRE should be made available in the pure rocket mode of flight. The LRE mass in the latter case may be the same as the LRE with deep-throttling. However, in both options there is a loss of efficiency: in the first option, due to the inevitable reduction in specific impulse, and in the second option, because of the increase in mass of the propulsion system.

Chosen Propulsion System. The basic propulsion system chosen consists of 12 DCTJ units

and three LRE units; two of the LRE units operate from take-off and the third one starts operation when the TJ is shut off. It may be pointed out that the overall throttle ratio when two LRE units are operating, each with ψ equal to unity, becomes 0.667. Thus in the beginning when the LRE units are throttled, the DCTJ unit contribution to the total thrust becomes increased; however, this also leads to an increase in specific mass of the propulsion system since the LRE units do not then fully contribute to the total thrust over the initial part of the flight.

In the current study, the LRE units have been assumed to be similar to the Japanese LE-7 engines with 86 tons of SLS thrust. Other units may be considered, for example the Russian RD-0120 with a reported throttling capability over the range 45 – 115%.

Payload Fraction as Performance Parameter

The main performance parameter selected for the assessment of different propulsion systems used for the SSTO vehicle is the difference in payload fraction between the simple LRE and the DCTJ-LRE propulsion scheme denoted by $\Delta\delta_{pp}$.

The payload fraction is defined as follows:

$$\Delta\delta_{pp} = \left[\left(m^C_{orb} - m^R_{orb}\right) - \left(m^C_{tank} - m^R_{tank}\right) - \left(m^C_{eng} - m^R_{eng}\right)\right] / m_o \qquad (9)$$

where m_{orb}, m_{tank}, and m_{eng} represent the orbital, tankage, and engine mass, respectively, and the superscripts C and R denote the case of the combined engine and the rocket, respectively. The initial mass of the vehicle is written as m_o.

Earlier in Ref. 5 a comparison was made between the simple LRE scheme and the DCTJ-LRE scheme with three LRE units, with either all or two units operated from the beginning of flight in different cases. In those cases, there was no oxygen injection. Figure 6 from that reference provides the payload fraction difference as a function of relative air flow k_A for different values of hydrogen distribution factor ξ; Fig. (6a) is for the case ψ = 1 and Fig. (6b) for the case ψ = 0.667, two of the LRE units operating in the latter case from the start. The figures also show the thrust limit, the dotted line in each, which indicates the limit beyond which the thrust-to-weight ratio cannot be greater than unity in the rocket mode of flight past the point of termination of the combined engine mode.

Comparing Figs. (6a) and (6b), it can be observed that the propulsion system with the LRE operating at full power from the start (ψ = 1.0) yields a somewhat higher efficiency than the throttled engine system (ψ = 0.667) at the same values of k_A and ξ. However, the payload fraction limit set by the thrust limit curve in Fig. (6a) is lower than that in Fig. (6b) by about 0.2% of the vehicle initial mass.

Another noteworthy feature is that the thrust limit curve in fact indicates the limits on the choice of one of k_A and ξ, given the other parameter and the payload fraction difference attainable. Also, the thrust limit curve indicates a maximum value for $\Delta\delta_{pp}$, and the values of k_A and ξ corresponding to that maximum represent the optimum choices for those parameters given the other system parameters.

Oxygen Injection Case. When oxygen injection is introduced, it is possible to vary, in addition to the parameters k_A and ξ, a third parameter, namely ϕ, the injected oxygen fraction in the air-oxygen mixture. Each value of ϕ, including ϕ = 0, yields a thrust limit curve. Thus the dotted lines shown in Fig. (6) can be assumed to pertain to ϕ = 0.

The analysis of the oxygen injection case has been carried out by determining the thrust limit curves for a series of values of ϕ. Figures (7a) and (7b), for ψ equal to 1.0 and 0.667, show the payload fraction improvement for several values of ϕ, including the case ϕ = 0, again as the difference between oxygen-augmented DCTJ-LRE scheme and the simple LRE scheme. Comparing Figs. 7a and 7b, it appears that throttling the LRE units leads to a small increase in payload fraction gain. In the full power case, the best improvement in payload fraction gain occurs at ϕ = 4%, while in the throttled LRE case the best improvement is found with ϕ = 8%. Generally the maximum moves towards a lower value of k_A with an increase in oxygen fraction. The best increase in payload fraction gain of 2.63% occurs at k_A = 14.0, ξ = 0.568, and ϕ = 8.3%. If ϕ = 0, that is in the case of no oxygen injection the best gain is 2.46% at k_A = 15.8 and ξ = 0.57. The best value in the full

power LRE operation is 0.29% lower as seen in Fig. 7a; however, the payload fraction difference between the oxygen case and the one without injection is only 0.02%.

Break-down of Payload Fraction Gain. Considering the throttled LRE case, Fig. 7b, an attempt has been made in Fig. 8 to provide the breakdown of the payload fraction gain in terms of the difference in mass of the principal elements of the flight vehicle as a per cent value of the initial mass of the vehicle; the specific cases considered are indicated by circles in Fig. 7b on the two thrust limit curves for $\phi = 0$ and $\phi = 8.0$. It can be observed in Fig. 8 that (a) the higher thrust of the oxygen-augmented DCTJ leads to a reduction in engine mass and this provides the major benefit in payload gain fraction; (b) the consumption of oxygen with the oxygen-augmented DCTJ is larger than the reduction in oxygen consumption of the LRE in the rocket mode, thus causing the payload gain fraction to reduce based on overall oxygen consumption; and (c) hydrogen consumption is reduced and this not only provides a compensation for the increased oxygen consumption but also a finite but small saving in the tankage mass.

Effect of LRE Choice on Combined Cycle Parameters. It must be pointed out here that in Ref. 12 it has been suggested that for a SSTO vehicle with LRE propulsion a thrust-to-weight ratio of 1.3 is optimal at take-off. However in the case of the combined DCTJ-LRE propulsion system, considering the thrust generation profile of the engines, a thrust-to-weight ratio of 1.5 seems necessary, and this is the value assumed in carrying out the analysis.

In the current study, the LRE chosen, the LE-7 engines, the vehicle had an initial mass of 400 tons. With a thrust-to-weight ratio of 1.5 at take-off, the thrust required is 600 tons. The two LE-7 engines with a combined throttle ratio of $\psi = 0.667$ provide a thrust of 172 tons, and the balance of the thrust must be obtained from the DCTJ engine. Thus, the initial thrust fraction of the total thrust required that has to be provided by the DCTJ cannot be selected arbitrarily when the LRE thrust output is fixed because of use of existing LRE engines.

Referring to Fig. 7b, the actual thrust fractions required when existing LRE are used are less than the optimal values indicated by circles. For the case of the LE-7 LRE, the modified thrust limits are indicated by the two filled squares. A comparison of the three choices, one, with LRE only, two, with the combined DCTJ-LRE, and three, with oxygen-augmented DCTJ-LRE, is given in Table 1.

General Conclusions

The oxygen-augmented DCTJ-LRE system provides a reduction in engine mass, hydrogen consumption, and tankage mass. Despite a decrease in specific impulse, and additional oxygen consumption, the oxygen-augmented combined cycle engine with thermally integrated LRE and DCTJ shows an improvement in payload fraction gain. In the specific case considered, the variation of specific impulse of the combined cycle engine and of the fraction of total thrust provided by the DCTJ engine are shown in Fig. 9 as a function of flight Mach number.

VEHICLE-ENGINE CONFIGURATION

In general, three applications are considered for the combined cycle engine: one, a SSTO vehicle with the combined DCTJ-LRE propulsion, two a SSTO vehicle with a detachable DCTJ booster, and three a TSTO with the combined DCTJ-LRE propulsion. In the latter case, considering a rocket of the type of H-2 or Ariane, it can be shown that there arises as much as 2.3 times increase in payload fraction, almost entirely due to a reduction in the vehicle initial mass. In particular for the case of H-2, the total mass of airbreathing boosters, including engines, fuel, and tankage, is estimated as 56 tons, compared to the 150 tons per solid booster.

A schematic of a SSTO vehicle with the basic combined cycle propulsion is presented in Fig. 10. A set of 12 DCTJ engines are included with a common intake and a common aerospike type of nozzle. The LRE nozzles are separate and are located in the core of the tail section.

The second of the applications considered, with a detachable airbreathing booster, is attractive in several ways. This concept provides considerable flexibility in the combined cycle configuration and operation. Preliminary estimates indicate a payload fraction gain of 3 – 5% over that of a SSTO rocket vehicle. For realizing the best benefits in cost, one must consider an airbreathing booster that is truly reusable. Figure 11 provides a schematic of a SSTO vehicle with a rocket of 400 ton gross weight and a detachable airbreathing booster. In this case 4 modules of boosters are installed with the core rocket. Each module includes propellant tanks, two DCTJ

engines with their own intakes and nozzles, and recovery and auxiliary systems; the propellant tanks carry hydrogen and oxygen required for the DCTJ and LRE operation up to the point of booster separation. Figure 12 shows the DCTJ configuration, and Table 2 provides the principal parameters of interest.

It appears that all of the engine parameters given in Table 2 are within conventional ranges, except for air temperature. It may be noted here that for an air temperature (downstream of the precooler) of 100 K (speed of sound being about 210 m/s), it is necessary to consider advanced design of compressors. The compressed air temperature is not higher than 400 – 450 K in any part of the regime, and therefore carbon fiber reinforced plastics or light alloys are indicated for compressor rotors.

CONCLUSIONS

The concept of a SSTO vehicle propulsion system with a thermally integrated LRE and DCTJ with oxygen injection in front of the (DCTJ) precooler appears attractive and feasible.

The problem of precooler icing can be overcome up to the desired flight altitude starting from SLS conditions at most acceptable launch sites. The chilling required in front of the precooler at SLS conditions is to 240 – 270 K. Oxygen addition can be terminated when the vehicle has reached a pre-assessed location along the flight trajectory.

An increase in vehicle performance – in terms of a payload gain fraction of about 0.15% of the initial mass – has been shown in the oxygen augmented case compared to the basic DCTJ-LRE case, but this is insignificant.

Compared to rocket propulsion the combined DCTJ-LRE propulsion yields a maximum increase in payload fraction of 2.63% of the vehicle initial mass.

The concept of oxygen-augmentation can be incorporated into a SSTO vehicle with a reusable airbreather. Such a vehicle is a low-risk development realizable within current capabilities. The operational costs of such a vehicle need further analysis.

Several other synergistic developments are feasible in the future.

REFERENCES

1. Balepin, V.V., Yoshida, M., and Kamijo, K., "Rocket Based Combined Cycles for Single Stage Rocket," SAE Paper 941166, 1994.
2. Escher, W.J.D. and Czysz, P.A., "Rocket-Based Combined-Cycle Powered Spaceliner Concept," Paper IAF-93-S.4.478, 1993.
3. Czysz, P.A., "Rocket Based Combined Cycle (RBCC) Propulsion Systems Offer Additional Options," XI International Symposium on Air Breathing Engines (ISABE), Tokyo, September 1993.
4. Ohkami, Y. and Maita, M., "Airbreathing Engine Selection Criteria for SSTO Propulsion System," *Transactions of the Japan Society for Aeronautical and Space Sciences*, Vol. 37, No. 118, 1995, pp. 239-247.
5. Balepin, V.V., Folomeev, E.A., Galkin, S.M., and Tjurikov, E.V., "Rocket Based Combined Cycles for Vertical Take-Off Space Vehicles," AIAA Paper 95-6078.
6. Billig, F.S., "Propulsion Systems from Takeoff to High-Speed Flight," High-Speed Flight Propulsion Systems, edited by S.N.B. Murthy and E.T. Curran, Vol. 137, Progress in Astronautics and Aeronautics, AIAA, Washington, DC, 1991, pp. 21-100.
7. Hewitt, F.A. and Johnson, M.C., "Propulsion System Performance and Integration for High Mach Air Breathing Flight," High-Speed Flight Propulsion Systems, edited by S.N.B. Murthy and E.T. Curran, Vol. 137, Progress in Astronautics and Aeronautics, AIAA, Washington, DC, 1991, pp. 101-142.
8. Rudakov, A.S. and Balepin, V.V., "Propulsion Systems with Air Precooling for Aerospaceplane," SAE Paper 911182.
9. Tanatsugu, N. et al., "Development Study on ATREX Engine," Paper IAF-94.5.4.428, 1994.
10. Balepin, V.V., Tanatsugu, N., Sato, T., Mizutani, T., Hamabe, K., and Tomike, J., "Development Study of Precooling for ATREX Engine," Proceedings of XII ISABE Symposium, 1995.
11. Maurice, L.Q., Leingang, J.L., and Carreiro, L.R., "Airbreathing Space Boosters Using In-Flight Oxidizer Collection," *AIAA Journal of Propulsion and Power*, July 1991.
12. Mansci, D. and Martin, J.A., "Evaluation of Innovative Rocket Engines for Single-Stage Earth-to-Orbit Vehicles," *AIAA Journal of Propulsion and Power*, Vol. 7, No. 6, Nov.-Dec. 1991, pp. 929-937.

Table 1. Comparison of the Three Vehicles

Vehicle	SSTO rocket with LRE propulsion	SSTO rocket with DCTJ/LRE propulsion	SSTO rocket with DCTJ/LRE propulsion, oxygen augmented DCTJ
Gross weight, tons	400	400	400
Initial thrust, tons	516	600	600
LRE thrust, tons	86 × 6	86 × 2 (+1)	86 × 2 (+1)
DCTJ thrust, tons		35.7 × 12	35.7 × 12
DCTJ thrust contribution, %		71.4	71.4
Air cooling ratio		15	14.2
Hydrogen distribution factor		0.538	0.524
Sea level specific impulse, m/s	3412	10210	8582
Engine mass, tons	9.11	20.78	18.84
Tanks mass, tons	13.67	14.88	14.77
Hydrogen mass, tons	50.62	60.00	59.19
Oxygen mass, tons	303.72	272.00	274.53
Initial airflow, kg/s		2292	2106
Vehicle volume, m^3	1092	1208	1198
Payload fraction benefit, %	basic level	+ 2.36	+ 2.49

Table 2. DCTJ Sea Level Parameters

	Basic DCTJ[5]	DCTJ augmented by oxygen
Thrust, tons	35.7	35.7
Specific impulse, m/s		
separately	51110	20260
integrated with LRE	10210	8580
Weight-to-thrust ratio, kg/ton		
separately	37.9	33.1
integrated with LRE	35.3	31.4
Airflow, kg/s	191	176
Hydrogen flow, kg/s		
through precooler	12.73	12.37
through combustors	6.85	6.48
Oxygen flow, kg/s	-	10.8
Air temperature in front of compr., K	110	104 - 110
Compressor pressure ratio	30	30
Turbine pressure ratio	1.7	1.7
Gas temperature in front of turbine, K	1700	1700

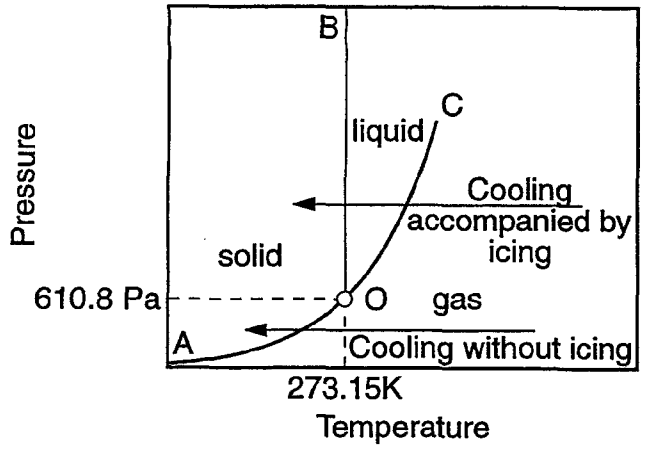

Figure 1. Thermodynamic Diagram for Water. AO - sublimation line; OB - solidification line; OC - saturation line.

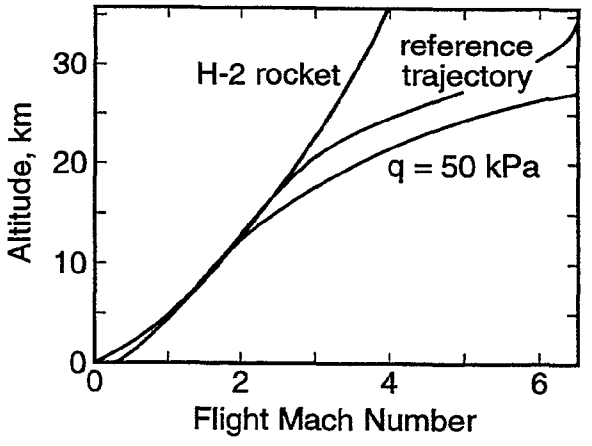

Figure 2(a). Reference Trajectory.

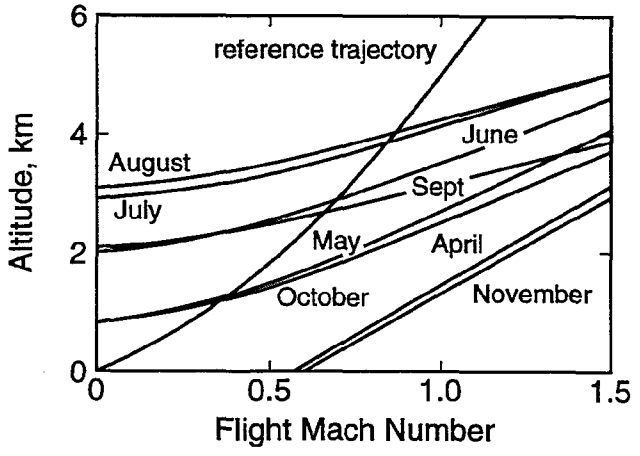

Figure 2(b). Seasonal Limits for Condensation.

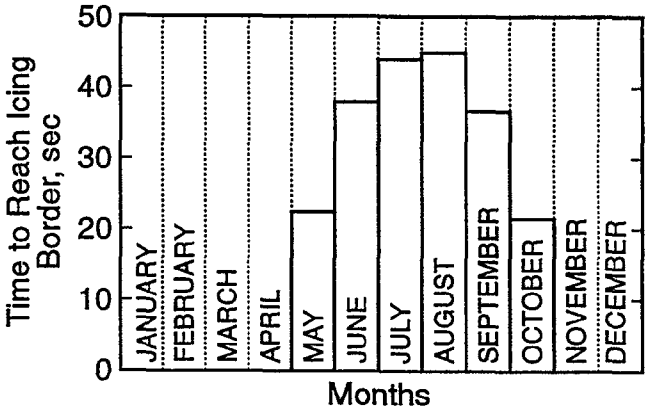

Figure 3. Length of Time of Oxygen Injection Required over Various Months

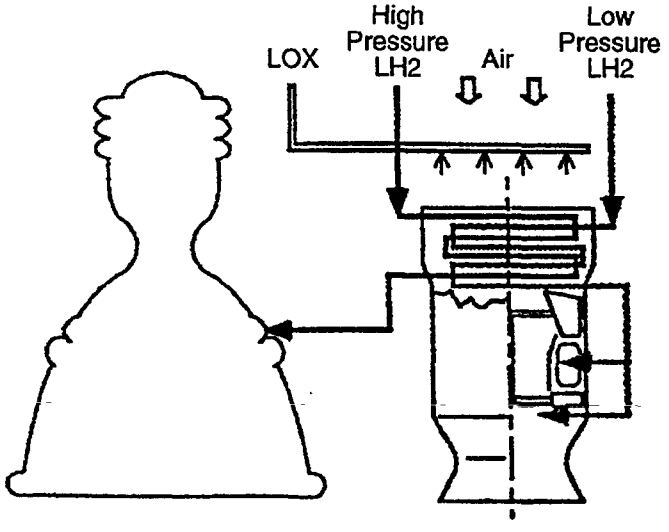

Figure 4. DCTJ-LRE Schematic.

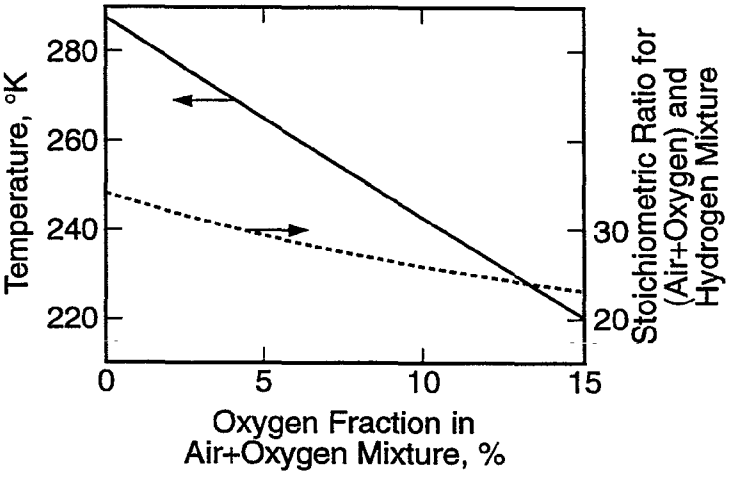

Figure 5. Temperature of Air-Oxygen Mixture and Stoichiometric Ratio as a Function of Oxygen Fraction Added.

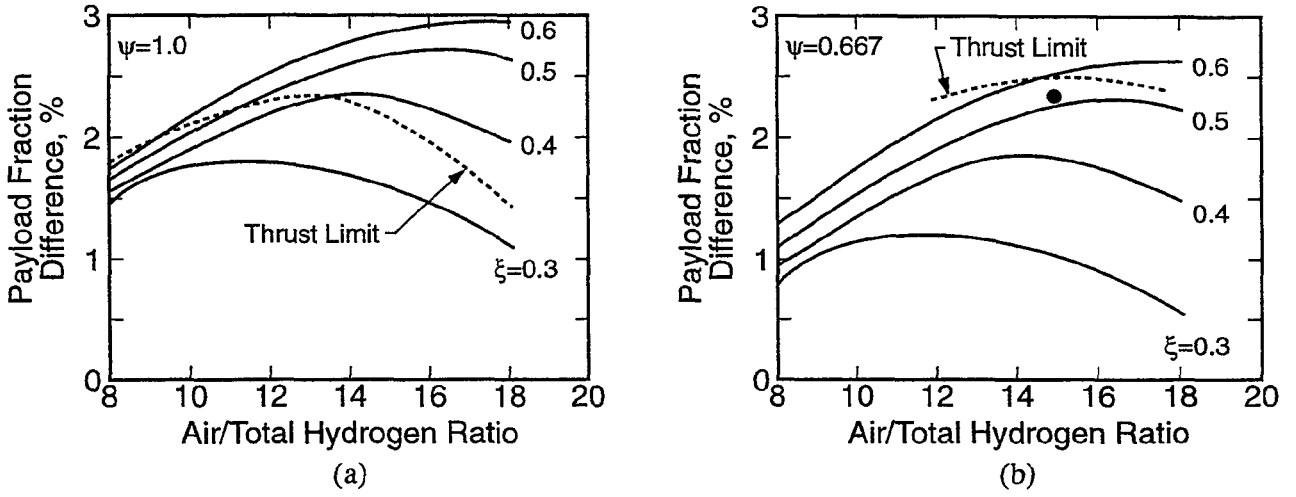

Figure 6. Payload Fraction Difference as a Function of Air/Toatl Hydrogen Ratio with ξ as a Parameter for (a) $\psi = 1.0$ and (b) $\psi = 0.667$.

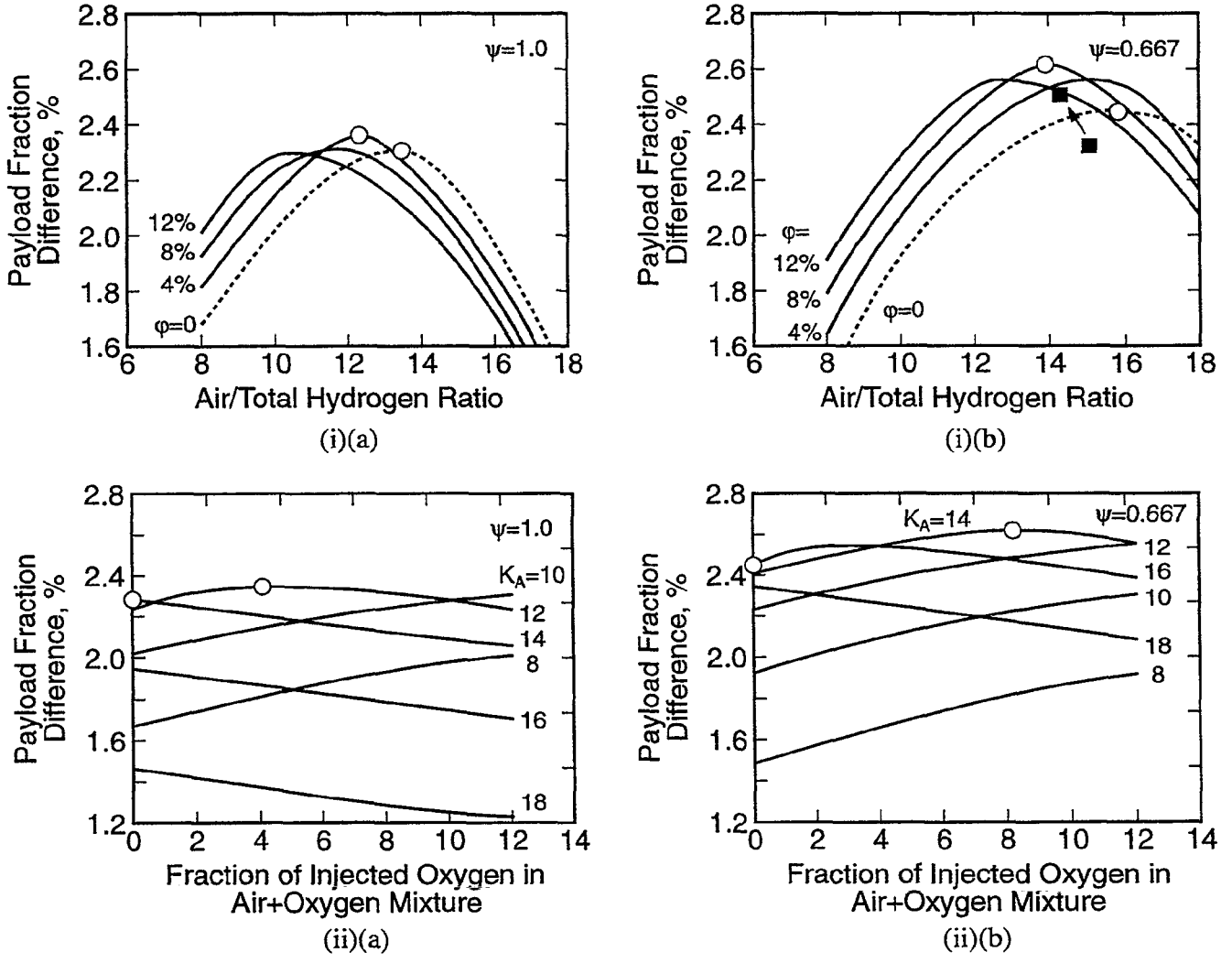

Figure 7. Payload Fraction Difference (i) as a Function of Air/Toatl Hydrogen Ratio with ϕ as a Parameter for (a) $\psi = 1.0$ and (b) $\psi = 0.667$ (ii) as a Function of Fraction of Injected Oxygen in Air-Oxygen Mixture with K_A as a Parameter for (a) $\psi = 1.0$ and (b) $\psi = 0.667$.

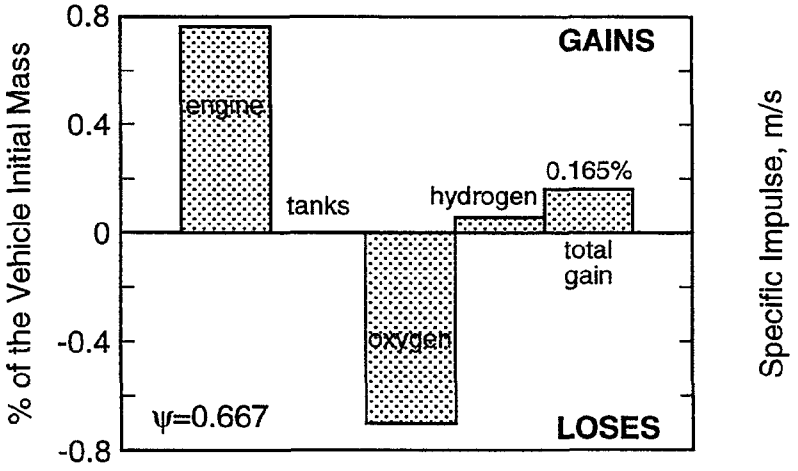

Figure 8. Breakdown of Initial Mass Corresponding to Figure 7(b).

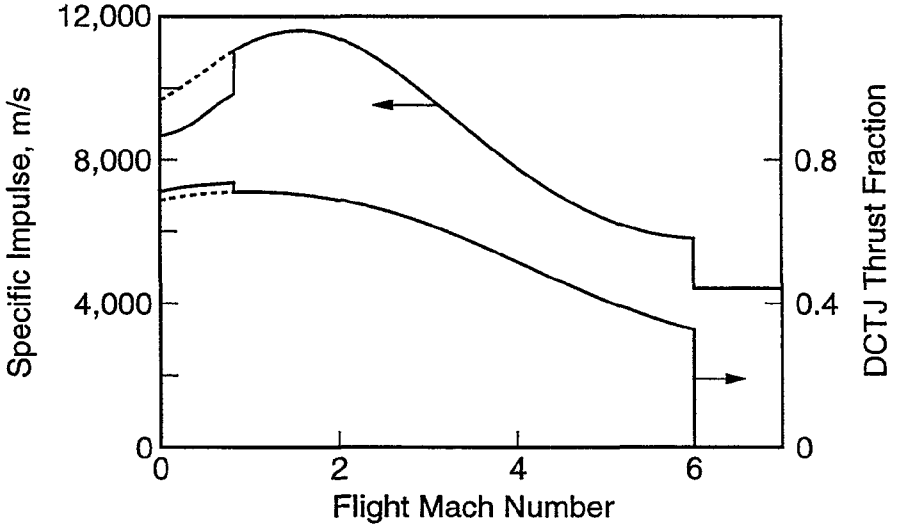

Figure 9. Specific Impulse and DCTJ Thrust Fraction as a Function of Flight Mach Number.

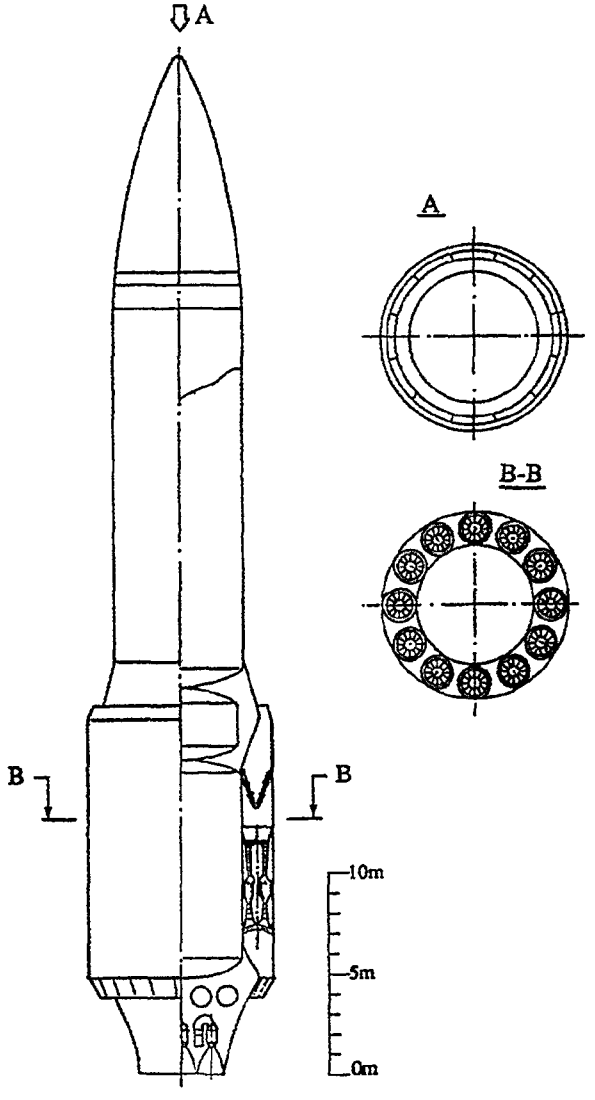

Figure 10. An SSTO Vehicle with Basic Combined Cycle Propulsion.

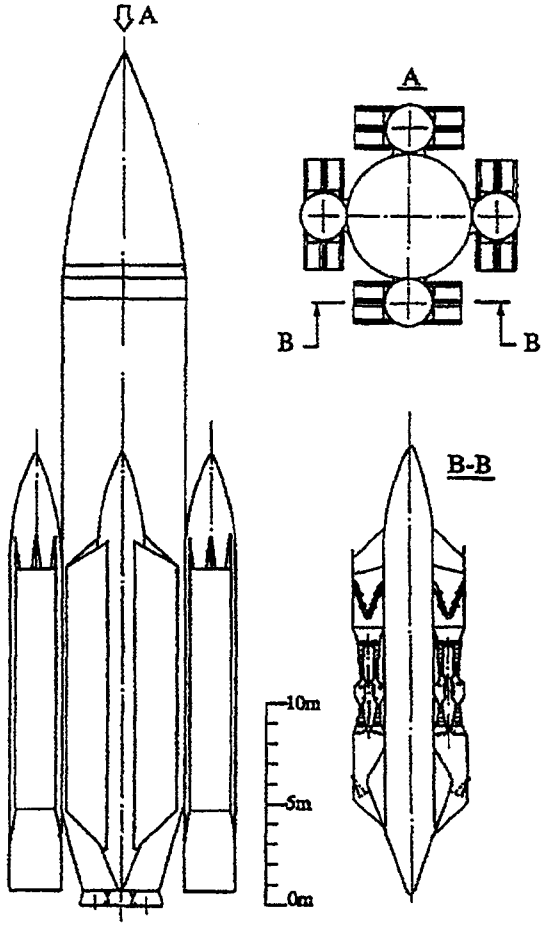

Figure 11. An SSTO Vehicle with Rocket Propulsion and a Detachable Airbreathing Booster.

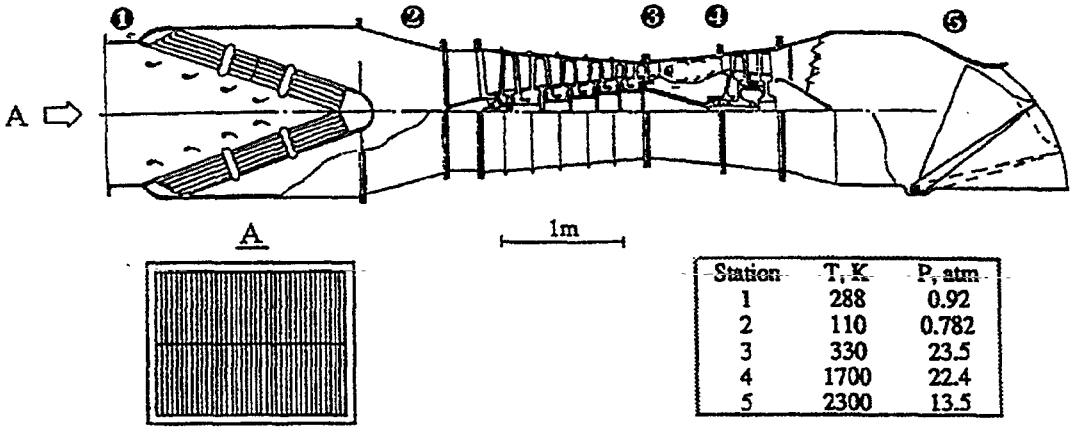

Station	T, K	P, atm
1	288	0.92
2	110	0.782
3	330	23.5
4	1700	22.4
5	2300	13.5

Figure 12. A DCTJ Configuration.